



## Development and Characterization of Mucoadhesive Microcapsules of Nateglinide: Ionic Orifice Gelation Technique

Santhosh Kumar Mankala\*<sup>1</sup>, Appanna Chowdary Korla<sup>2</sup>, Sammaiah Gade<sup>3</sup>

<sup>1</sup>Department of Pharmaceutics, Vaageswari College of Pharmacy, Karimnagar, Andhra Pradesh, India.

<sup>2</sup>Department of Pharmaceutics, Roland Institute of Pharmaceutical Sciences, Khodasingh, Berhampur, Orissa, India.

<sup>3</sup>Department of Pharmaceutical Chemistry, University College of Pharmaceutical Sciences, Kakatiya University, Warangal, Andhra Pradesh, India.

\*Corresponding author: [inspiration.santosh@gmail.com](mailto:inspiration.santosh@gmail.com)

### ABSTRACT

Type-2 diabetes is a metabolic disorder where the body is unable to automatically regulate blood glucose levels, resulting in hyperglycemia because the pancreatic  $\beta$ -cell does not produce enough insulin. This produces the classical symptoms of Polyuria (frequent urination), polydipsia (increased thirst) and polyphagia (increased hunger). Nateglinide is a meglitinide short-acting non-sulfonylurea, pancreatic, beta-cell-selective, KATP potassium channel blocker that improves overall glycemic control in type-2 diabetes. Nateglinide binds rapidly to the sulfonylurea SUR<sub>1</sub> receptor with rapid association and dissociation gives nateglinide a unique "fast on-fast off" effect. Nateglinide has short biological half-life of 1.5-2.5 h and therefore a sustained release medication is required to get prolonged effect and to reduce fluctuations in drug plasma concentration levels. Microencapsulation is an accepted process used to achieve controlled release and drug targeting for many years. Mucoadhesion has been a topic of interest in the design of drug delivery systems to prolong its intestinal residence time. Mucoadhesion facilitates the intimate contact of the dosage form with the underlying absorption surface for improved bioavailability of drugs. Nateglinide microcapsules were prepared employing SA (sodium alginate) as the coat material in combination with some mucoadhesive polymers such as (sodium carboxy methylcellulose) Sod. CMC and (methyl cellulose) MC (drug:SA:polymer at ratios 2:2:1, 2:3:1 and 2:4:1) following orifice-ionic gelation technique. Infrared (IR) spectroscopy, differential scanning calorimetry and X-ray diffraction studies proved the compositions were compatible without any interaction between the drug and excipients. The prepared microcapsules were evaluated for various physical and release parameters. The resulted microcapsules were found to be discrete and spherical in scanning electron microscopy studies and free flowing in rheological studies. The size of microcapsules was found to be around  $756.54 \pm 19.276 \mu\text{m}$  to  $797.12 \pm 14.761 \mu\text{m}$ . The microencapsulation efficiency and swelling index was found to be higher in Sod. CMC than in MC containing formulations. The microcapsules with MC exhibited good mucoadhesive property in the *in vitro* wash-off test. *In vitro* drug release studies of nateglinide microcapsules were carried out up to 24 h and they followed zero-order release kinetics with Super case II mechanism. The drug release from the microcapsules was sustained over a prolonged period with greater retardation in drug:SA:Sod.CMC (2:4:1) containing microcapsules and this proved to be the best formulation.

**Keywords:** Nateglinide, controlled release, ionic-orifice gelation, microencapsulation, mucoadhesion.

### 1. INTRODUCTION

Diabetes is a clinically and genetically heterogeneous group of disorders/metabolic disorder affecting the metabolism of carbohydrates, lipids, and proteins. The characteristic feature of diabetes is an abnormal elevation in blood glucose levels (Hyperglycemia), is due to a deficiency of insulin secretion caused by pancreatic  $\beta$ -cell dysfunction and/or insulin resistance in liver and muscle. Diabetes is a syndrome in which chronic hyperglycemia leads to long-term damage to various organs including the heart, eyes, kidneys, nerves, and vascular system. This high blood sugar produces the classical symptoms

of Polyuria (frequent urination), polydipsia (increased thirst) and polyphagia (increased hunger). This metabolic dysregulation is often associated with alterations in adipocyte metabolism. The current classification of diabetes is based upon the pathophysiology of each form of the disease. Type-1 diabetes results from cellular mediated autoimmune destruction of pancreatic b-cells, usually leading to total loss of insulin secretion. Type-1 diabetes is usually present in children and adolescents, although some studies demonstrated 15% to 30% of all cases being diagnosed after 30 years of age. The lack of insulin production in patients with type-1 diabetes makes the use of exogenous insulin necessary to sustain life, hence the

former name "insulin-dependent diabetes." In the absence of insulin, these patients develop ketoacidosis, a life-threatening condition. Type-2 diabetes, previously called non-insulindependent diabetes, results from insulin resistance, which alters the use of endogenously produced insulin at the target cells. Type-2 patients have altered insulin production as well; however, autoimmune destruction of b-cells does not occur as it does in type-1, and patients retain the capacity for some insulin production. Because the type-2 patient still produces insulin, the incidence of ketoacidosis is very low compared to type-1 as insulin secretion becomes insufficient to compensate for insulin resistance. Although type-2 patients do not need insulin treatment to survive, insulin is often taken as part of the medical management of type-2 diabetes [1].

Nateglinide is a metglinide short-acting, pancreatic, beta-cell-selective, KATP potassium channel blocker that improves overall glycemic control in type-2 diabetes. Although nateglinide's mechanism of action is related to that of sulphonyl-ureas, important differences do exist. Nateglinide binds rapidly to the sulphonylurea SUR<sub>1</sub> receptor with a relatively low affinity, and it dissociates from it extremely rapidly in a manner of seconds. This rapid association and dissociation gives nateglinide a unique "fast on-fast off" effect. Thus, nateglinide has a rapid onset and short duration of action on beta cells in stimulating insulin secretion *in vivo* and providing good control of postprandial hyperglycemia when taken immediately prior to meals. This hypoglycemic effect of nateglinide leads to improved glycemic control, while the short duration avoids delayed hyperinsulinemia and hypoglycemia after meals. Nateglinide is not a sulphonylurea, but it shares the mechanism of action of commonly used oral hypoglycemic agents such as glibenclamide and glipizide. Like the recently introduced, short-acting agent, repaglinide, it does not incorporate a sulphonylurea moiety. Compounds with such a profile should not only achieve improved overall glucose control, but also reduce the risk of vascular complications which is the most important feature of nateglinide. Nateglinide is both effective and well tolerated in the treatment of type-2 diabetes. The reported overall profile of adverse effects appears to be superior to that of other KATP potassium channel blockers, the glucose modulator metformin and PPAR- $\gamma$  agonists such as troglitazone. Clinical comparisons of these agents have shown nateglinide to be more effective in attenuating postprandial glucose than any other oral hypoglycemic agent, and that treatment with nateglinide provides effects that afford improved control of plasma glucose levels. The administration regimen for nateglinide, immediately prior to meals, also facilitates patient compliance [2].

Several studies have reported on controlled drug delivery systems in the form of tablets, films, patches, and gels for oral, buccal, nasal, ocular, and topical routes. Nateglinide is made available as many forms in the market like conventional and

simple sustained release tablets, but microencapsulation is a technique used to deliver the medicament at controlled rate by targeting. Microcapsules have more advantages over conventional and simple sustained release tablet formulations, such as targeting, less dosing frequency, zero-order release and high margin of safety, which are not possible with the existing formulations. Amongst the polymers used for microencapsulation, alginate has gained much attention since it is non toxic, biodegradable and can be prepared by a safe technique avoiding organic solvents. Hence orifice-ionic gelation technique was developed as an alternative approach even though so many other techniques are available like single and double emulsification techniques, normal and interfacial polymerization, coacervation phase separation, spray drying, spray congealing, etc. [3].

Microcapsules can be defined as solid, approximately spherical particles made of polymeric, waxy or other protective materials ranging in size from 1 to 1000  $\mu\text{m}$ . Microencapsulation is a process used to achieve controlled release and drug targeting. Mucoadhesion has been a topic of interest in the design of drug delivery systems to prolong the residence time of the dosage form in (gastrointestinal tract) GIT, which facilitates the intimate contact with the absorption surface to enhance the bioavailability of drugs [4]. Mucoadhesion is the process by which a natural or a synthetic polymer can be adhered to a (biological substrate) mucosal layer, and the phenomenon is known as mucoadhesion. The substrate possessing mucoadhesive property can help in devising a delivery system capable of delivering a drug for a prolonged period of time at a specific delivery site and offers several advantages over other oral controlled systems by virtue of prolongation of residence of the drug in GIT. Mucoadhesive microcapsules provide the needed continuous therapy in the management of type-2 diabetes with high margin of safety by evaluating pre- and post-formulation parameters [5-6].

There are numerous drugs for treating type-2 diabetes, The objective of the present work was to develop, characterize (pre- and post-formulation parameters) and evaluate nateglinide mucoadhesive microcapsules by following orifice-ionic gelation technique using (Sod. Alginate) SA as the release rate retarding polymer, with (sodium carboxy methylcellulose) Sod. CMC and (methylcellulose) MC as mucoadhesive polymers. Sod. CMC, and MC are economic and easily available synthetic hydrophilic polymers, and these can be extensively used for designing mucoadhesive delivery systems due to their ability to exhibit strong hydrogen bonding with the mucin present in the mucosal layer as compared to thiolated polymers, lectin-based polymers and other natural polymers. Basically, polymers of natural source containing polysaccharides, carbohydrates and cystine are be less stable as compared to those containing synthetic polymers as these are highly prone for microbial degradation [7].

## 2. MATERIALS AND METHODS

Nateglinide pure drug was obtained as a gift sample from M/s Hetero Drugs Ltd., Hyderabad, (AndhraPradesh, India). Sod. CMC and MC were procured from M/s Central Drug House (P) Ltd., (New Delhi, India). SA (having a viscosity of 5.5 cps in a 1% w/v aqueous solution at 25°C), calcium chloride and petroleum ether were procured from M/s S. D. Fine Chemicals Pvt. Ltd., Mumbai, (Maharashtra, India).

### 2.1. Preparation of Nateglinide Mucoadhesive Microcapsules

Nateglinide mucoadhesive microcapsules were prepared by employing SA as the coat material in combination with four mucoadhesive polymers such as Sod. CMC and MC (drug:SA:polymer at ratios 2:2:1, 2:3:1 and 2:4:1) by following orifice-ionic gelation process. SA (2.0 g, 3.0 g and 4.0 g) and the mucoadhesive polymer (1.0 g) were dissolved in purified water (25 ml) to form a homogenous polymer solution to which core material; nateglinide (2.0 g) was added and mixed thoroughly to get smooth viscous dispersion (Table 1).

The resulting dispersion was then added drop wisely into 100 ml calcium chloride (10% w/v) solution through a syringe with a needle of No. 22 size. The added droplets were retained in the calcium chloride solution for 15 min to complete the curing reaction and to produce spherical rigid microcapsules. The microcapsules were separated by decantation and the product was washed with water and petroleum ether and dried at 45° C for 12 h. [8-10]. The stated ratios were fixed as per the results obtained in manual optimization of SA and mucoadhesive polymer. When drug:SA:polymer was less than 2:2:1, the formulation was found to disintegrate within a short time, and when the ratio was more than 2:4:1, the dosage form weight was increased to more than 1100 mg, making it difficult to fill in a capsule and the release was also retarded for more than 24 h. When the ratio of mucoadhesive polymer was decreased less than the fixed ratio formulations became non-adhesive, and when it was increased more than the fixed ratio, all the microcapsules became sticky and this also led to drying problem.

Table 1: Composition of various batches of nateglinide mucoadhesive microcapsules

S. No	Ingredients	Qty used in formulations (g)					
		NSM <sub>1</sub>	NSM <sub>2</sub>	NSM <sub>3</sub>	NMM <sub>4</sub>	NMM <sub>5</sub>	NMM <sub>6</sub>
1.	Nateglinide	2	2	2	2	2	2
2.	Sod. Alginate	2	3	4	2	3	4
3.	Sod. CMC	1	1	1	-	-	-
4.	MC	-	-	-	1	1	1
<b>Total Weight</b>		5	6	7	5	6	7
<b>Drug:SA:Polymer</b>		2:2:1	2:3:1	2:4:1	2:2:1	2:3:1	2:4:1

### 2.2. Evaluation of Prepared Microcapsules

#### 2.2.1. Particle size analysis

All the batches prepared were analyzed for particle size where the microcapsules were placed on a set of standard sieves ranging from sieve No. 16# to 60#, using an electromagnetic sieve shaker (Electro Lab, EMS-8). The sieves were arranged in such a way that they were in a descending order with the mesh size 16# on the top and 60# mesh in the bottom. The microcapsules passed through the set of sieves and the amount retained on each sieve was weighed and the average mean diameter was determined and considered as mean particle size [11]:

$$\text{Mean Particle Size} = \frac{\sum(\text{Mean Particle Size of the Fraction} \times \text{Weight Fraction})}{\sum(\text{Weight Fraction})} \dots (1)$$

#### 2.2.2. Bulk density

Accurately weighed microcapsules (M) were transferred into a 100 ml graduated cylinder to measure the apparent volumes or bulk volume (V<sub>b</sub>). The measuring cylinder was tapped for a fixed period of time and tapped volume (V<sub>t</sub>) occupied in the cylinder was measured. The bulk density and tapped/true density were calculated in gram per milliliter by the following formula [12]:

$$\text{Bulk Density}(\rho_b) = \frac{\text{Weight of Microcapsules(g)}(M)}{\text{Bulk Volume (ml)}(V_b)} \dots (2)$$

$$\text{True/Tapped Density}(\rho_t) = \frac{\text{Weight of Microcapsules(g)}(M)}{\text{Tapped Volume (ml)}(V_t)} \dots (3)$$

Where, M = mass of the powder, V<sub>b</sub> = bulk volume of the powder and V<sub>t</sub> = tapped volume of the powder.

### 2.2.3. Carr's index and Hausner's ratio

The static angle of repose was measured according to the fixed funnel and free standing cone method. The bulk density of the mixed microcapsules was calculated for determining the Hausner's ratio and Carr's index from the poured and tapped bulk densities of a know weight of sample using a measuring cylinder [13-14]. The following equations were used for the calculations:

$$\text{Carr's Index} = \left[ \frac{\text{Tapped Density} - \text{Bulk Density}}{\text{Tapped Density}} \right] \times 100 \dots (4)$$

$$\text{Hausner's Ratio} = \frac{\rho_T}{\rho_B} \dots (5)$$

### 2.2.4. Angle of repose

A funnel was fixed in a stand in such a way that the top of the funnel was at a height of 6 cm from the surface. The microcapsules were passed from the funnel so that they formed a pile. The height and the radius of the heap were measured and the angle of repose was calculated using the equation [12, 15].

$$\theta = \text{Tan}^{-1} \left[ \frac{h}{r} \right] \dots (6)$$

### 2.2.5. Scanning Electron Microscopy (SEM)

The surface, morphology, microcapsules size, microcapsules shape, etc., were determined by using Scanning Electron Microscopy (BIOMETRICS: SEM-CS491Q/790Q). Dry microcapsules were placed on an electron microscope brass stub that was coated with gold (thickness 200 nm) in an ion sputter. Pictures of microcapsules were taken by random scanning of the stub under the reduced pressure (0.001 torr).

### 2.2.6. % Drug content evaluation

Nateglinide content in the microcapsules was estimated by UV-spectrophotometric method at a wavelength of 227 nm in phosphate buffer of pH 7.4, with 10% methanol (Elico, SL-158). The method obeyed Beer's law in the concentration range 10-50 µg/ml. Microcapsules containing equivalent to 100 mg of nateglinide were crushed as fine powder, extracted with 10 ml of methanol, and made up to 100 ml with pH 7.4 phosphate buffer. One milliliter of the sample solution was taken and made up to the volume to 10 ml with phosphate buffer pH 7.4, and the absorbance was measured at wavelength 227 nm. The procedure was repeated with pure nateglinide. The absorbance values from the pure drug nateglinide and microcapsules were treated and the %drug content was calculated. The method was validated for linearity, accuracy and precision.

### 2.2.7. Microencapsulation efficiency

Microencapsulation efficiency was calculated using the following formula [16]:

$$\text{Microencapsulation efficiency} = \left[ \frac{\text{Estimated percentage drug content}}{\text{Theoretical percentage drug content}} \right] \times 100 \dots (7)$$

### 2.2.8. Determination of wall thickness

Wall thickness of microcapsules was determined by using the equation [17]:

$$h = \frac{\Gamma(1-P)d_1}{3(Pd_2 + 1 - P)d_1} \dots (8)$$

Where, h = wall thickness,  $\Gamma$  = arithmetic mean radius of microcapsules,  $d_1$  and  $d_2$  are densities of core and coat material respectively, and P is the proportion of medicament in microcapsules. All the experimental units were studied in triplicate (n = 3).

### 2.2.9. Swelling index

Pre-weighed nateglinide microcapsules ( $W_0$ ) formulated with mucoadhesive polymers by employing different coat: core ratios were placed in pH 7.4 phosphate buffer maintained at 37°C. After the 3<sup>rd</sup> hour, the microcapsules were collected and blotted to remove excess water and weighed ( $W_t$ ). The swelling index was calculated with the following formulae [18]:

$$\text{Swelling Index} = \frac{W_t - W_0}{W_0} \times 100 \dots (9)$$

where  $W_t$  = weight of microcapsules observed at the 3<sup>rd</sup> h and  $W_0$  = the initial weight of microcapsules.

### 2.2.10. Permeability studies

The permeability constant  $P_m$  of the microcapsules was calculated using the equation [19]:

$$P_m = \frac{K \cdot V \cdot H}{A \cdot C_s} \dots (10)$$

Where, V is the volume of the dissolution medium ( $\text{cm}^3$ ), H the wall thickness of the microcapsules (mm), A the surface area of the microcapsules ( $\text{cm}^2$ ),  $C_s$  the solubility of the core material (mg) in the dissolution medium and K is the release rate constant ( $\text{mg}/\text{h}^{-1}$  or  $\text{h}^{-1}$ ).

For a given microcapsule and under standard testing conditions the values of V, A and  $C_s$  remains constant and hence the equation can be written as:

$$P_m = K \times H \dots (11)$$

where K is the release rate constant and H is the wall thickness of the microcapsule.

### 2.2.11. Fourier Transform Infrared studies

Fourier Transform Infrared (FT-IR) analysis measurements of pure drug, carrier and drug-loaded microcapsules formulations were obtained using a Perkin-Elmer system 200FT-IR spectrophotometer. The pellets were prepared on KBr-press under a hydraulic pressure of 150 kg/cm<sup>2</sup>; the spectra were scanned over the wave number range of 4000-400 cm<sup>-1</sup> at the ambient temperature.

### 2.2.12. Differential scanning calorimetry (DSC)

Differential scanning calorimetry (DSC) was performed on nateglinide drug loaded microcapsules using Seiko (Japan) DSC model 220C. Samples were sealed in aluminum pans and the DSC thermograms were reported at a heating rate of 10°C/min from 20 to 260°C.

### 2.2.13. X-ray diffraction studies

Different samples were evaluated by X-ray powder diffraction. Diffraction patterns were obtained using X-ray diffractometer with a radius of 240 mm. The Cu Ka radiation was Ni filtered. A system of diverging and receiving slits of 1 and 0.1mm respectively was used. The pattern was collected with 40 kV of tube voltage and 30 mA of tube current and scanned over the 2 $\Theta$  range of 10<sup>o</sup>-80<sup>o</sup>.

### 2.2.14. In vitro wash-off test for mucoadhesive microcapsules

The mucoadhesive property of the microcapsules was evaluated by an *in vitro* adhesion testing method known as wash-off method. A piece of goat intestinal mucus (2 × 2 cm) was mounted onto glass slides of (3 × 1 inch) with elastic bands. Glass slide was connected with a suitable support. About 50 microcapsules were spread onto each wet tissue specimen, and thereafter the support was hung onto the arm of a USP tablet disintegrating test machine (Electro Lab, ED 2AL). The disintegration machine containing tissue specimen was adjusted for a slow, regular up and down moment in a test fluid at 37°C taken in a beaker. At the end of 1 h and later at hourly intervals up to 8 hours, the machine was stopped and the number of microcapsules still adhering onto the tissue was counted. The test was performed in phosphate buffer of pH 6.8 [20].

### 2.2.15. In vitro drug release studies of microcapsules

*In vitro* drug release studies of microcapsules were carried out using USP XXIII Eight station dissolution rate test apparatus Type I with a basket stirrer (Electro Lab, EDT 08 LX) at 100 rpm in 900 ml 0.1 N HCl for the 1<sup>st</sup> 2 h, then in phosphate buffer of pH 7.4 at 50 rpm and temperature 37 ± 0.5°C. Microcapsules equivalent to 100 mg of nateglinide were

tied in a muslin bag and kept in the basket. Five milliliter samples of the dissolution fluid were withdrawn at regular intervals and replaced with fresh quantity of dissolution fluid. The samples were filtered, diluted and analyzed, using Elico, SL-158 Double-beam UV-Visible Spectrophotometer at wavelength 221 and 227 nm respectively. For all the formulations, the dissolution was carried out in triplicates and statistically analyzed using InStat3®. The obtained data were used to calculate the % drug release and to determine the order and mechanism of the release [21]. The formulation that showed best release was prepared 6 times and 3 samples from each batch were evaluated for drug release and the results were statistically analyzed by analysis of variance (one factor ANOVA) [22].

### 2.2.16. Curve fitting analysis [23-26]

#### Zero-order release rate kinetics

To study the zero-order release kinetics, the release rate data are fitted to the following equation:

$$Q = K_0 t \dots (12)$$

where “Q” is the fraction of drug released, “K” the release rate constant and “t” is the release time.

#### First-order kinetics

A first-order release would be predicated by the following equation:

$$\text{Log } C = \text{Log } C_0 - \frac{Kt}{2.303} \dots (13)$$

where; C = amount of drug remaining at time “t”, C<sub>0</sub> = initial amount of the drug and K = first-order rate constant (h<sup>-1</sup>)

When the data are plotted as cumulative percent drug remaining versus time, it yields a straight line, indicating that the release follows first-order kinetics. The constant “K” can be obtained by multiplying 2.303 with slope.

#### Higuchi release model

To study the Higuchi release kinetics, the release rate data were fitted to the following equation:

$$Q = K.t^{1/2} \dots (14)$$

where, “Q” is the amount of drug released, “K” the release rate constant, and “t” is the release time.

When the data are plotted as accumulative drug released versus square root of time, it yields a straight line, indicating that the drug was released by diffusion mechanism. The slope is equal to “K”.

*Korsmeyer-peppas release model*

The release rate data were fitted into the following equation,

$$Mt/M_{\infty}(Q) = K.t^n \dots (15)$$

where,  $Mt/M_{\infty}$  is the fraction of drug released, "K" is the release constant, "t" is the release time, and "n" is the diffusion exponent for the drug released that is dependent on the shape of the matrix dosage form.

When the data are plotted as log of drug released versus log time, it yields a straight line with a slope equal to "n" and the "K" value can be obtained from Y intercept:

$$Q = Kt^n \dots (16)$$

When n approximates 0.5, a Fickian/diffusion control release

is implied: where  $0.5 > n < 1$ , it implies non-Fickian transport; and  $n = 1$  for zero-order release.

**3. RESULTS AND DISCUSSION**

The SEM and sieve analysis results showed the microcapsules to be discrete, spherical and free flowing. The particle size of microcapsules was found to be between  $756.54 \pm 19.276 \mu\text{m}$  and  $797.12 \pm 14.761 \mu\text{m}$  with an average size of  $776.83 \pm 17.018 \mu\text{m}$  (Figure 1). Angle of repose, bulk density, Carr's index and Hausner's ratio were found to be between  $24.41 \pm 0.749$  and  $27.74 \pm 0.515$ ,  $0.498 \pm 0.166$  and  $0.580 \pm 0.103$ ,  $12.99 \pm 4.765$  and  $19.96 \pm 3.578$ , and  $1.1492 \pm 0.0787$  and  $1.2493 \pm 0.0436$ , respectively (Table 2).

**Table 2: Physical parameters data of nateglinide mucoadhesive microcapsules NSM<sub>1</sub>-NMM<sub>6</sub>**

Formulation	Angle of Repose	Bulk Density (g/cm <sup>3</sup> )	Carr's Index	Hausner's Ratio	Mean Particle Size (μm)	Wall Thickness (μm)	Permeability coefficient (μm/hr)
NSM <sub>1</sub>	27.74±0.515	0.58 ±0.103	19.96±3.578	1.2493±0.0436	756.54±19.276	88.51 ±2.983	577.164
NSM <sub>2</sub>	24.93 ±0.52	0.512±0.0757	17.056±4.536	1.2056±0.0787	782.34±23.234	98.843±3.762	554.815
NSM <sub>3</sub>	24.41±1.202	0.542±0.0452	14.364±2.869	1.1677±0.0546	797.12±14.761	106.492±3.543	520.106
NMM <sub>4</sub>	24.93±0.302	0.498 ±0.166	14.344±4.675	1.1674±0.0435	758.9 ±18.127	88.791 ±2.961	590.62
NMM <sub>5</sub>	24.41±0.749	0.532±0.0972	15.944±1.979	1.1896±0.0768	770.6 ±33.849	97.365 ±4.552	587.062
NMM <sub>6</sub>	27.11±0.202	0.565±0.0632	12.99 ±4.765	1.1492±0.0787	785.4 ±29.556	104.929±5.873	579.963

\*Mean ± S.D (n=3)

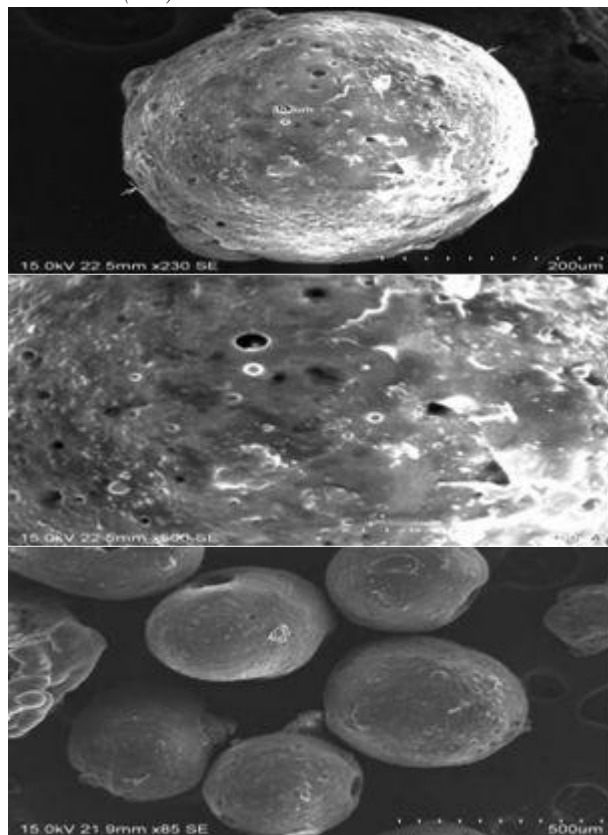


**Figure 1: SEM pictograms of nateglinide mucoadhesive microcapsules prepared with Sod.CMC**

Drug excipient compatibility was proved by FT-IR spectroscopy, DSC and X-ray diffraction (XRD) studies. In the IR spectra of nateglinide, the pure drug formed a number of peaks prominently at different wave numbers, indicating the presence of functional groups like carboxyl, carbonyl and amino groups like peaks at  $1701 \text{ cm}^{-1}$  and  $1724 \text{ cm}^{-1}$  wave number were due to C-C and C=O stretching in aliphatic chain and ester. Prominent peaks at  $1643 \text{ cm}^{-1}$ ,  $1296 \text{ cm}^{-1}$ , and  $1446 \text{ cm}^{-1}$  were appeared due to C=O stretching, C-O stretching and, C-O-H stretching in acidic group and peak at  $1215 \text{ cm}^{-1}$  wave number as stretching in aliphatic chain indicated the presence of carboxylic group and keto group in the structure. Broad peaks appeared between  $2950 \text{ cm}^{-1}$  and  $2850 \text{ cm}^{-1}$  wave number were due to C=C stretching in aromatic structure. Peaks appearing at  $2931 \text{ cm}^{-1}$  and  $1408 \text{ cm}^{-1}$  were because of C-H stretching aromatic and in  $\text{CH}_3$  and  $\text{CH}_2$  aliphatic respectively. A more intense peak was found between  $3296 \text{ cm}^{-1}$  and  $3311 \text{ cm}^{-1}$  because of N-H stretching indicating the presence of amino group in the structure and peak at  $1384 \text{ cm}^{-1}$  wave number also indicates the presence of C-N stretching. Peak at  $1624 \text{ cm}^{-1}$  was appeared because of -C-O-C stretching in SA. And, all these peaks were appeared unchanged in IR spectra of combinations like nateglinide + SA + Sod. CMC and nateglinide + SA + MC. The above interpretational data clearly states no interaction between the

pure drug nateglinide and other excipients. Therefore, it can be said that the drug and excipients are compatible (Figure 2).

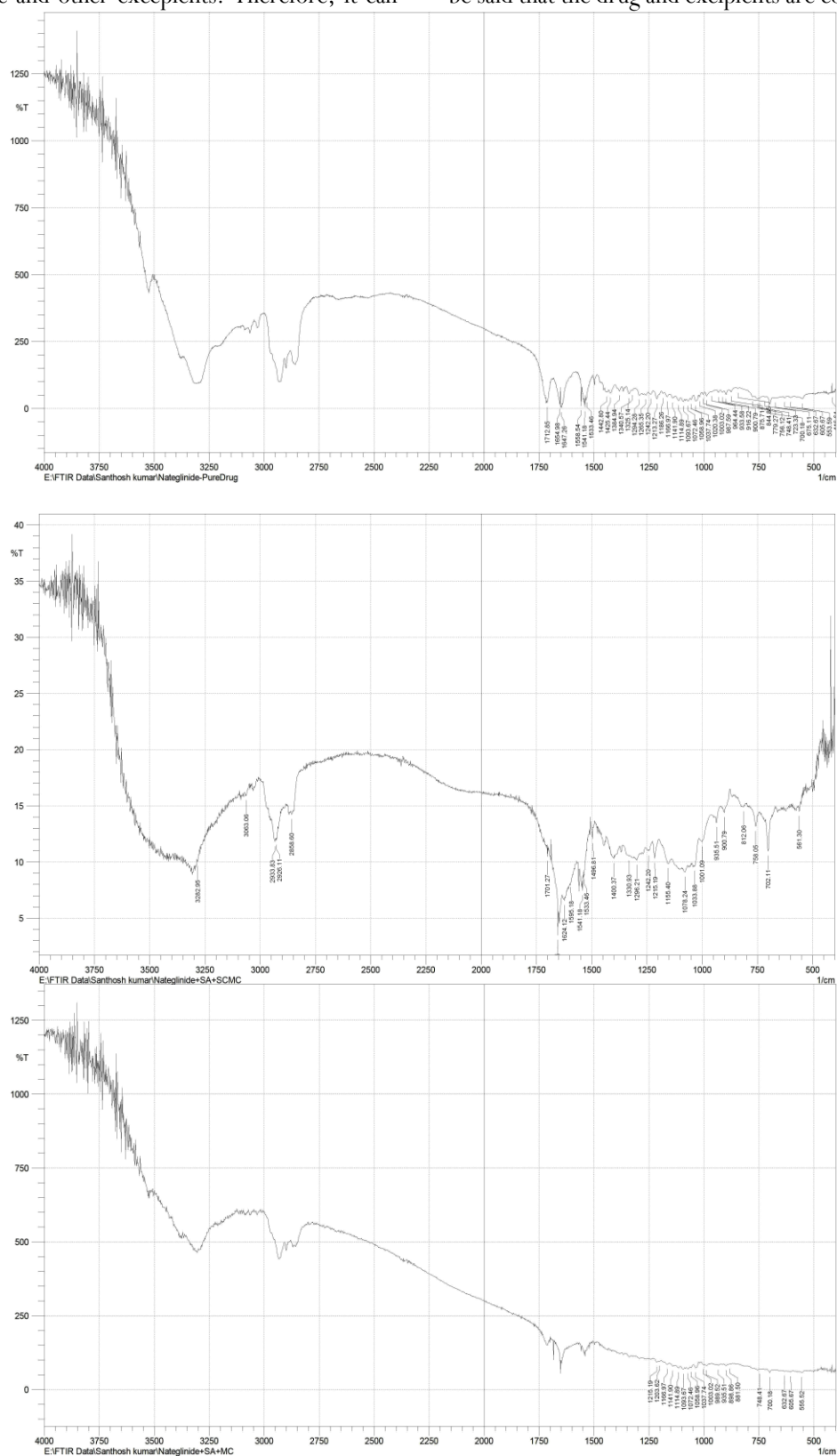


Figure 2: FT-IR spectra of nateglinide pure drug, nateglinide+SA+Sod.CMC and nateglinide+SA+MC.

The melting point of pure nateglinide was found to be 135.78 °C and followed endothermic type of reaction for which the onset was at 126.30°C and ended at 138.85 °C. The glass

transition lag was found around 12.50°C and the same endothermic type of reactions was found in all combinations like nateglinide + SA + Sod. CMC and nateglinide + SA +

MC. No change was found in the melting point as well as glass transition lag, but special peaks were found indicating melting point of SA as 219.93°C, Sod. CMC as 109.71°C and MC as 101.97°C, and the influence of excipients was found to be only in changing on's and end's sets of melting point peaks of nateglinide by absorbing heat but not by interactions. The above interpretational data clearly indicate that the crystalline nature of the drug had not been changed and it did not undergo any polymorphism because there was no interaction, which has been proved by its unchanged melting point in all the combinational spectra. X-ray diffractogram of nateglinide proves its crystalline nature as evidenced from the number of sharp and intense peaks. The diffractogram of nateglinide with polymers showed diffused peaks indicating amorphous nature of the polymers and sharp, intense peaks indicating the crystalline nature of drug. Diffraction pattern of drug with polymer mixture showed simply the sum of the characteristic peaks of polymer indicating the presence of drug in crystalline form. Diffraction patterns of sample spectra represent the availability of crystalline peaks of drug situated at 12.83, 16.55, 20.01, 21.45, 25.76 and 38.21 (2θ) similar to the pure drug with corresponding intensities and linear counts respectively. The obtained 2θ values as characteristic peaks were found at the same position in combinations like nateglinide + SA + Sod. CMC and nateglinide + SA + MC, but the intensities got reduced because of diffused peaks and more orientation in case of polymers. The reduction in intensities or linear counts of peaks in combinations was possibly due to decrease in the degree of crystallinity of the drug that might have occurred when the drug is well dispersed in the SA + polymer matrix. Finally the DSC and XRD data indicate that the crystallinity of pure drug was unchanged and stable, and indirectly show that the compositions are compatible. (Figures 3 and 4).

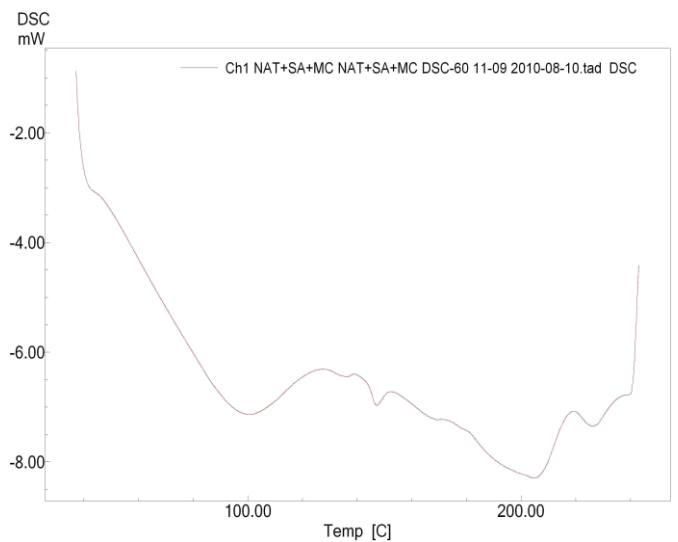
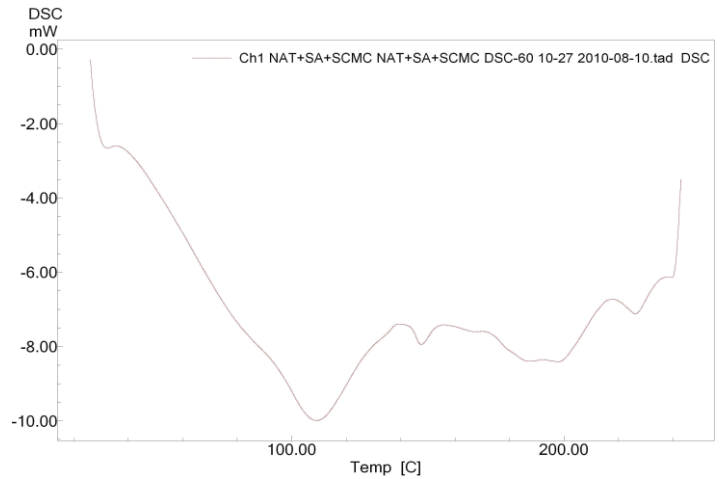
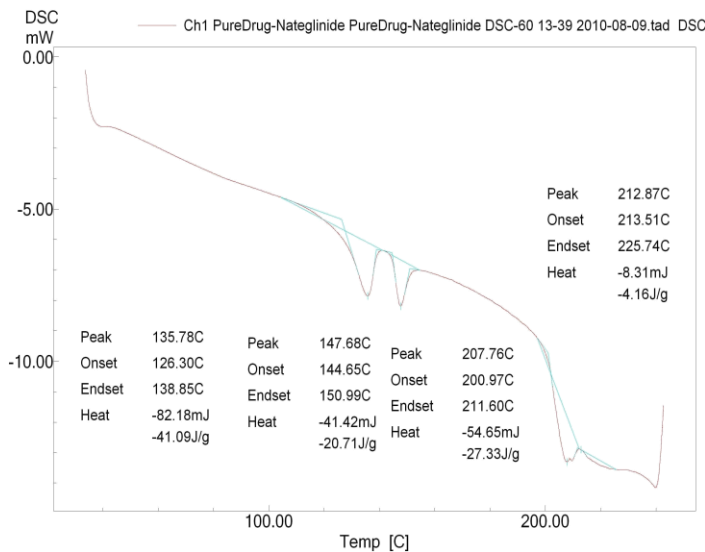


Figure 3: DSC spectra of nateglinide pure drug, nateglinide+SA+Sod.CMC and nateglinide+SA+MC



The microencapsulation efficiency was from  $80.892 \pm 7.275$  to  $93.878 \pm 4.356\%$  with practical % drug content values around  $22.65 \pm 3.165$  to  $36.55 \pm 2.254\%$  (Table 3). Wall thickness and permeability coefficient were found around  $88.51 \pm 2.983$  to  $106.492 \pm 3.543 \mu\text{m}$  and  $520.106$  to  $590.62 \mu\text{g/h}$ , respectively. Swelling index was the highest in formulation NSM<sub>3</sub> around  $189.29 \pm 13.553\%$  w/w and the least in NMM<sub>4</sub> around  $57.89 \pm 12.554\%$  w/w (Figure 5). All microcapsules exhibited good mucoadhesive property in the *in vitro* wash-off test (Figure 6) and microcapsules with MC NMM<sub>5</sub> showed better mucoadhesion where 24% of microcapsules were found adhered to the mucosal layer after 8 h (Table 4). In the *In vitro* drug release studies, the highest release retardation was found to be around  $98.7697 \pm 2.0964\%$  in formulation NSM<sub>3</sub> up to 22 h whereas the least retardation was observed to be around  $99.6677 \pm 3.8762\%$  in the formulation NMM<sub>4</sub> after 16 h (Figure 7). When that the best formulation was prepared 6 times (batches) and, three

samples from each batch were taken then evaluated for drug release ( $n = 3$ ) and statistically analyzed by (one factor ANOVA), the data showed  $Df_1$  (5) and  $Df_2$  (30) with an F-value of 1.4714. The obtained F-value found less than  $f$ -table value around 3.68 indicating less difference in between the groups

and within the groups.  $P$ -value was found to be significant around 0.2609, proving maximum closeness between the results. All formulations followed zero-order non-Fickian release kinetics with Super Case II Transport mechanism (Table 5).

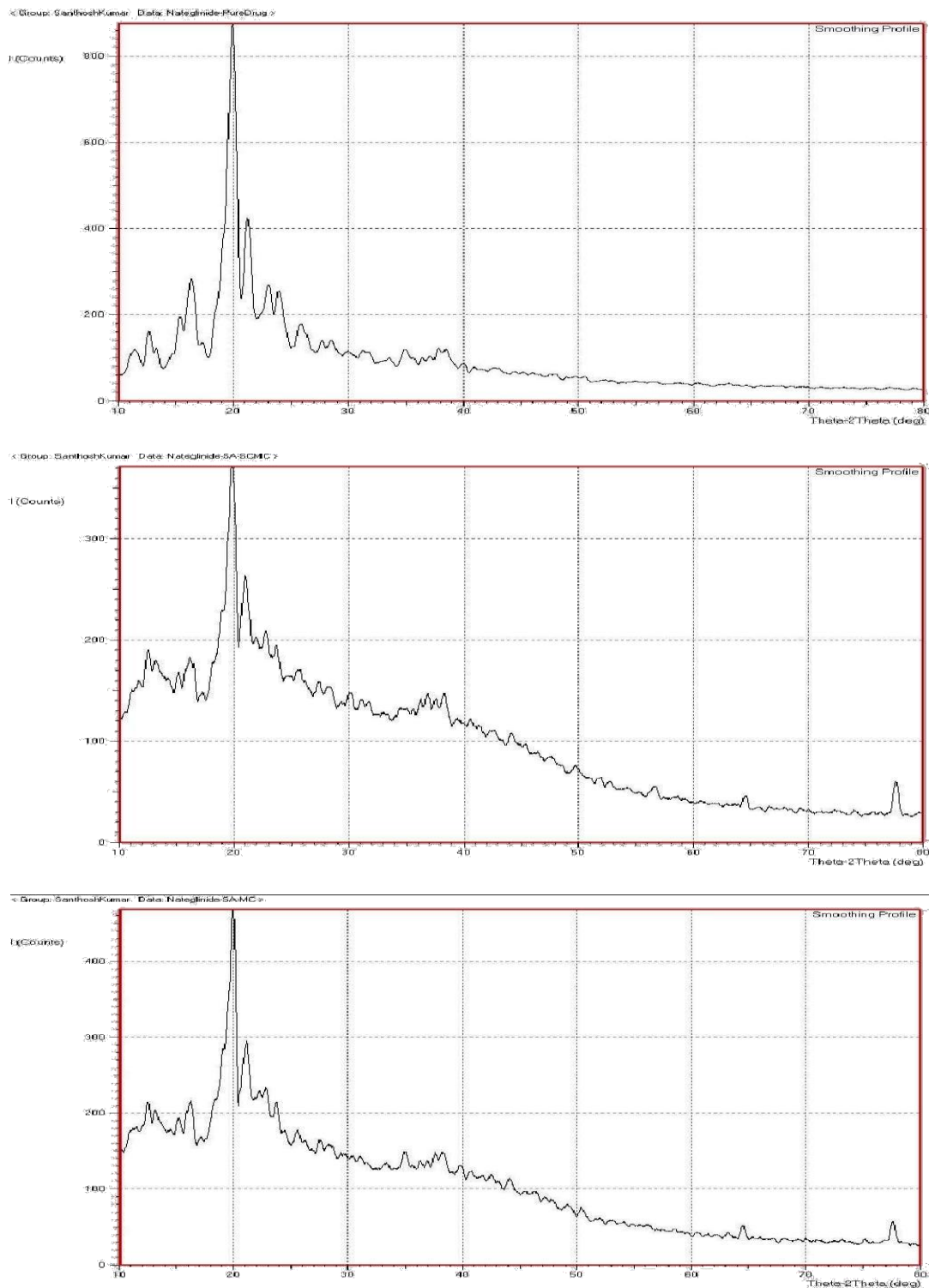


Figure 4: X-Ray diffraction spectra of nateglinide pure drug, nateglinide+SA+Sod.CMC and nateglinide+SA+MC

Table 3: Drug content / Encapsulation Efficiency of formulations NSM<sub>1</sub>-NMM<sub>6</sub>

Formulation	D:SA:P ratio	Weight Taken (mg)	Theoretical Drug content (mg)	Practical Drug Content (mg)	Encapsulation Efficiency (%)
NSM <sub>1</sub>	2:2:1	100	40	36.55 ± 2.254	91.375 ± 5.126
NSM <sub>2</sub>	2:3:1	100	33.33	30.98 ± 1.975	93.878 ± 4.356
NSM <sub>3</sub>	2:4:1	100	28.57	25.36 ± 1.991	90.571 ± 4.198
NMM <sub>4</sub>	2:2:1	100	40	34.58 ± 2.321	86.45 ± 6.124
NMM <sub>5</sub>	2:3:1	100	33.33	30.24 ± 1.012	91.636 ± 2.448
NMM <sub>6</sub>	2:4:1	100	28.57	22.65 ± 3.165	80.892 ± 7.275

\*Mean ± S.D (n=3)

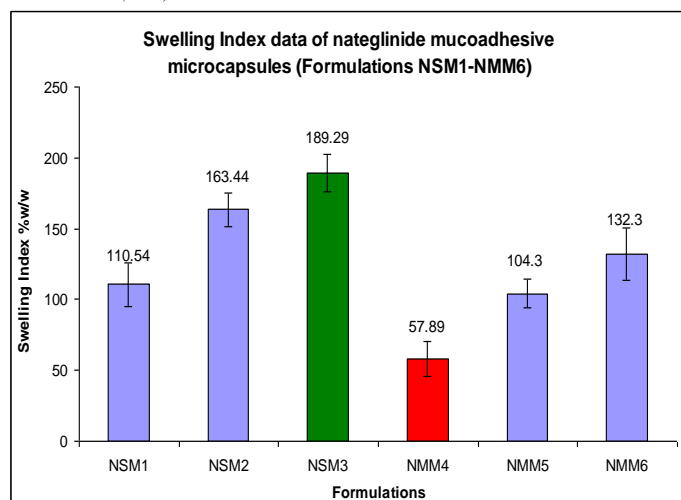


Figure 5: Swelling Index histogram of nateglinide mucoadhesive microcapsules NSM<sub>1</sub>-NMM<sub>6</sub>

All physical parameters were found in the acceptable range. The microencapsulation efficiency and swelling index were found to be greater with Sod. CMC than in other formulations, whereas mucoadhesive efficiency was found higher in formulations with MC. All compositions were found compatible in IR, DSC and XRD studies and thus are suitable for extending the scope of work in this research area. The drug release from the microcapsules was sustained over an

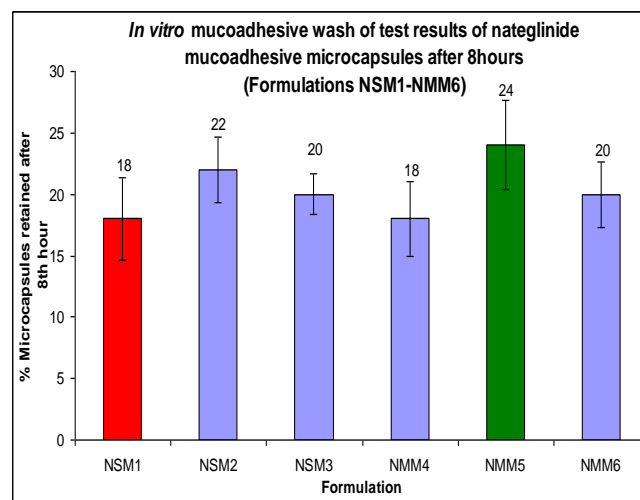


Figure 6: In vitro mucoadhesive wash off test results histogram of nateglinide mucoadhesive microcapsules NSM<sub>1</sub>-NMM<sub>6</sub> after 8 h

extended period of time. The study states that release depended on the core: coat ratio and type of mucoadhesive agent, which got retarded as the coat material percentage got increased. Microcapsules prepared using Sod. CMC showed better sustained action, and formulation containing drug: SA: Sod. CMC in the ratio 2:4:1 was found to be the best formulation as it released the maximum drug up to 22 h.

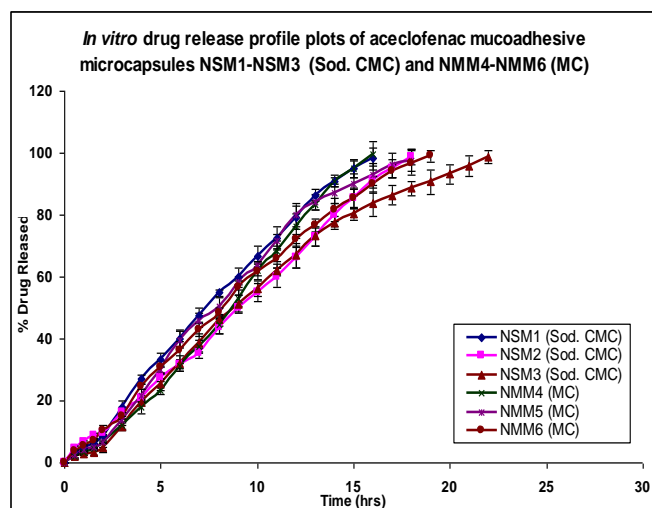
Table 4: In Vitro Wash off Test Data of formulations NSM<sub>1</sub>-NSM<sub>6</sub>

Formulation (50 microcapsules)	% of microcapsules (±SD) adhering to tissue at (h) Phosphate buffer, pH 7.4			
	1	2	4	8
NSM <sub>1</sub>	52 ± 4.66	44 ± 2.66	34 ± 2	18 ± 3.33
NSM <sub>2</sub>	68 ± 5.33	56 ± 4	44 ± 3.33	22 ± 2.66
NSM <sub>3</sub>	82 ± 5	68 ± 4.33	58 ± 4.66	20 ± 1.66
NMM <sub>4</sub>	52 ± 3.33	44 ± 4.33	34 ± 2.66	18 ± 3
NMM <sub>5</sub>	62 ± 2.66	56 ± 2.66	43 ± 3.33	24 ± 3.66
NMM <sub>6</sub>	76 ± 4.66	62 ± 4	48 ± 2.66	20 ± 2.66

\*Mean ± S.D (n=3)

Table 5: Release Kinetic Data of Formulations NSM<sub>1</sub>-NMM<sub>6</sub>

Formulation	Zero Order	Release rate constant	First Order	Higuchi	Best Fit	Korsmeyer-Peppas		Release Mechanism
	r <sup>2</sup>	K <sub>0</sub>	r <sup>2</sup>	r <sup>2</sup>		r <sup>2</sup>	n value	
NSM <sub>1</sub>	0.9952	6.5209	0.8519	0.9462	Zero order	0.9859	1.086	Super Case II
NSM <sub>2</sub>	0.9981	5.6131	0.7844	0.9297	Zero order	0.9871	0.9335	Super Case II
NSM <sub>3</sub>	0.9759	4.884	0.8918	0.9611	Zero order	0.9778	1.1674	Super Case II
NMM <sub>4</sub>	0.9933	6.6518	0.6893	0.9019	Zero order	0.9941	1.2334	Super Case II
NMM <sub>5</sub>	0.9828	6.0295	0.9146	0.9483	Zero order	0.9827	1.1442	Super Case II
NMM <sub>6</sub>	0.991	5.5272	0.8374	0.9587	Zero order	0.9916	0.9973	Super Case II

Figure 7: In vitro drug release plots of nateglinide mucoadhesive microcapsules NSM<sub>1</sub>-NMM<sub>6</sub>

#### 4. CONCLUSION

The mucoadhesive microencapsulation by following orifice-ionic gelation technique could be adopted in the laboratory as well as in the industry, as it is simple and reproducible. In conclusion, MC and Sod. CMC microcapsules could be used for better mucoadhesive action and SA could be used for better sustained action over an extended period of time. Release retardation depends not only on coat material percentage but also on mucoadhesive polymer selected. However, further *in vivo* studies are needed to optimize the drug for sustained action in human beings for better bioavailability, and efficacy, and thus safety.

#### 5. ACKNOWLEDGEMENTS

Authors wish to thank M/s Hetero Drugs Ltd., Hyderabad, (Andhra Pradesh India) for providing gift sample of Nateglinide, and authors will be thankful to management of Vaageswari College of Pharmacy, Karimnagar, (Andhra Pradesh, India) for supporting us to finish up this study successfully.

#### 6. REFERENCES

- Mealey BL, Oates TW. *J Periodontol*, 2006; **77(8)**:1289-1303.
- Norman P, Rabasseda X. *Drugs Today*, 2001; **37(6)**:411-426.
- Solmaz D, Reza A, Mohammadreza A and Ramin K. *African J Pharm Pharmacology*, 2010; **4(6)**:346-354.
- Robinson RJ, Lee VH. *Controlled Drug Delivery: Fundamentals and Applications*. Revised and expanded. Vol 29; 2nd ed. New York: Marcel Dekker Inc; 2005. p. 9-19.
- Boddupalli BM, Mohammed ZNK, Ravinder Nath A, Banji D. *J Adv Pharm Tech Res*, 2010; **1**: 381-387.
- Pranshu TSK, Sathish MNV. *Int J Pharma Bio Sci*, 2011; **2(1)**: 458-467.
- Carvalho FC, Bruschi ML, Evangelista RC, Gremiao MPD. *Brazilian J Pharm Sci*, 2010; **46(1)**: 1-17.
- Chowdary KPR, Srinivas L. *Indian Drugs*, 2000; **37**: 400-410.
- Liu XD, Yu WY, Zhang Y, Xue WM, et al. *J Microencapsulation*, 2002; **18**: 775-782.
- Bahadur S, Chanda R, and Roy A, *Res J Pharm Tech*, 2008; **1(2)**: 100-105.
- Lachman L, Lieberman HA, Kanig JL. *The theory and practice of industrial pharmacy*. 3<sup>rd</sup> ed. Bombay: Varghese Publishing House; 1987. p. 22-28.
- Puttewar TY, Kshirsagar MD, Chadewar AV, Chikale RV. *J King Saud Uni*, 2010; **22**: 229-240.
- Hausner HH. *Int J Metall*, 1967; **3**: 7-13.
- Carr RL. *Chem Eng*, 1965; **72**: 163-168.
- Aulton ME. *Pharmaceutics: The Science of Dosage Form Design*. 3rd ed. New York: Churchill Livingstone; 1988: p. 605-613.
- Zinutti C, Hoffman M. *J Microencapsul*, 1994; **11(5)**: 555-563.
- Si-Nang L, Carlier PF, Delort P, Gazzola J, et al. *J Pharm Sci*, 1973; **62(3)**: 452-455.
- Ma XJ, Xie YB, Zhou L, Yu XJ, Yuan Q, Li CC, et al. *Chinese J Organ Transplantation*, 1995; **16**: 156-157.
- Koida Y, Kobayashi M, Samejima M. *Chem Pharma Bull*, 1986; **34(8)**: 3354-3361.

20. Lehr CM, Bowstra JA, Tukker JJ, Junginer HE. *J Control Rel*, 1990; **13(1)**: 51-62.
21. Costa P, Jose-Manuel SL. *Eur J Pharma Sci*, 2001; **13**: 123-133.
22. Yadav A, Jain DK. *J Adv Pharm Tech Res*, 2011; **2**: 51-55.
23. The Indian Pharmacopoeia, Vol-II, Indian Pharmacopoeia Commission, Ghaziabad, 2007. p. 740-742.
24. Higuchi T. *J Pharm Sci*, 1963; **52**: 1145-1149.
25. Ritger PL, Peppas NA. *J Controlled Rel*, 1987; **52**: 37-42.
26. Sipemann J, Peppas NA. *Adv Drug Del Rev*, 2001; **(48)**:139-157.